Crystallographic Evidence of a Transglycosylation Reaction: Ternary Complexes of a Psychrophilic α-Amylase[†,‡]

Nushin Aghajari,[§] Michel Roth,[#] and Richard Haser*[,§]

Institut de Biologie et Chimie des Protéines, UMR 5086 CNRS and Université Claude Bernard Lyon 1, Laboratoire de Bio-Cristallographie, 7 Passage du Vercors, 69367 Lyon Cedex 07, France and Laboratoire de Cristallographie et Cristallogénèse des Protéines, Institut de Biologie Structurale Jean-Pierre Ebel, 41 Jules Horowitz, 38027 Grenoble Cedex 1, France

Received December 18, 2001; Revised Manuscript Received January 30, 2002

ABSTRACT: The psychrophilic *Pseudoalteromonas haloplanctis* α-amylase is shown to form ternary complexes with two α-amylase inhibitors present in the active site region, namely, a molecule of Tris and a trisaccharide inhibitor or heptasaccharide inhibitor, respectively. The crystal structures of these complexes have been determined by X-ray crystallography to 1.80 and 1.74 Å resolution, respectively. In both cases, the prebound inhibitor Tris is expelled from the active site by the incoming oligosaccharide inhibitor substrate analogue, but stays linked to it, forming well-defined ternary complexes with the enzyme. These results illustrate competition in the crystalline state between two inhibitors, an oligosaccharide substrate analogue and a Tris molecule, bound at the same time in the active site region. Taken together, these structures show that the enzyme performs transglycosylation in the complex with the pseudotetrasaccharide acarbose (confirmed by a mutant structure), leading to a well-defined heptasaccharide, considered as a more potent inhibitor. Furthermore, the substrate-induced ordering of water molecules within a channel highlights a possible pathway used for hydrolysis of starch and related poly- and oligosaccharides.

α-Amylases (α-1,4-glucan-4-glucanohydrolase, EC 3.2.1.1) are endo-acting enzymes that catalyze the hydrolysis of α-1,4-glycosidic bonds in starch, glycogen, and related poly- and oligosaccharides. They are among the most industrially important enzymes, having wide applications, such as in brewing, starch-processing, textile, alcohol production, and detergent industries (*1*−*3*).

The bacterial *Pseudoalteromonas haloplanctis* α-amylase (hereafter AHA)[1] formerly known as *Alteromonas haloplanctis*, like other psychrophilic (cold loving) enzymes, operates optimally at temperatures close to 0 °C where the activity of mesophilic and thermophilic counterparts is drastically reduced, if not abolished (*4*). It shows a surprisingly high degree of homology in sequence (around 55% identity) as well as in tertiary structure with mammalian α-amylases and insect α-amylases (*4*−*7*). The crystal structures of native and Tris complexed AHA determined to 2.0 and 1.85 Å resolution, respectively (*6*), showed that AHA displays an overall topology common with all known structures of α-amylases from other species.

Interestingly, this psychrophilic α-amylase like its mammalian and at least one of its insect counterparts (*8*), is also chloride activated (*4*, *9*, *10*). At the structural level, an explanation for the allosteric activation of AHA by chloride has been given and may be valid for all chloride-dependent α-amylases (*6*, *12*, *13*). It is worth mentioning that α-amylases can serve as target molecules for studies of designed inhibitors used in diabetes, hyperlipaemia, and obesity treatments (*14*−*19*). Some of the oligosaccharide compounds used in these studies and in the above-mentioned treatments originate from the trestatin family, and several three-dimensional studies of α-amylases in complex with compounds from this family have been carried out (*20*−*28*). The most popular of these compounds, a pseudo-tetrasaccharide inhibitor, acarbose, is now marketed in many countries for use in the treatment of diabetes, and more than one reason causes the high interest of studying its interaction with α-amylases. For example, in the light of mechanistic studies this tetrasaccharide is interesting not only because of its properties as inhibitor, but also because it has been shown that several amylolytic enzymes in the crystalline state, when in contact with acarbose-like molecules, seem to be able to catalyze transglycosylation reactions resulting in different reaction products, the latter depending on the origin of the enzyme (*20*, *21*, *23*, *25*−*27*).

In this paper, we report the determinations of the crystal structures of two ternary complexes of AHA: one with acarbose (Figure 1a) and a Tris molecule, a second with Tris and the so-called component II (Figure 1b), which corresponds to the pseudo-trisaccharide derived from acarbose by removing its glucose reducing unit. In the presence of

[†] This work and N.A. were supported by the European Biotech program "COLDZYME" and the TMR program "COLDNET".

[‡] Coordinates for the structure described in this paper have been deposited with the Protein Data Bank (accession numbers 1G94, 1G9H, and 1KXH).

* Corresponding author: Tel: 33 (0) 4 72722608; fax: 33 (0) 4 72722616; e-mail: r.haser@ibcp.fr.

[§] CNRS Lyon.

[#] Grenoble.

[1] Abbreviations: AHA, *Pseudoalteromonas haloplanctis* α-amylase; PPA, porcine pancreatic α-amylase; Tris, 2-amino-2-(hydroxymethyl)-1,3-propanediol.

10.1021/bi0160516 CCC: $22.00 © 2002 American Chemical Society
Published on Web 03/06/2002

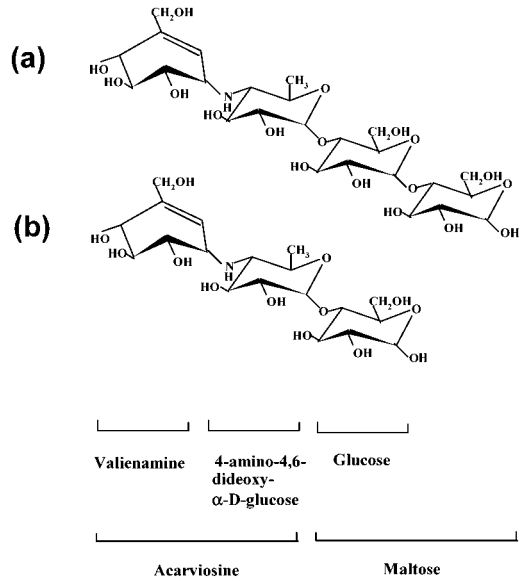

FIGURE 1: Structure of (a) acarbose, a drug for the treatment of diabetes, and (b) component II, a pseudo trisaccharide obtained by the cleavage of a glucose moiety from the reducing end of acarbose. The acarviosine unit formed by the valienamine ring linked to the "amino sugar" ring confers to the acarbose-like compounds their inhibitory effects.

acarbose and a high concentration of organic solvent, we show that AHA performs a transglycosylation reaction resulting in a well-defined heptasaccharide product. Remarkably, the structure of AHA complexed with acarbose reveals a channel, containing a series of well-defined water molecules, running from the surface through the enzyme and pointing toward the catalytic site. We furthermore report the crystal structure of a complex between an inactive mutant and acarbose, where the nucleophilic aspartic acid (Asp 174) has been mutated to an Asn, and which proves the ability of this cold adapted α-amylase of performing transglycosylation in the crystalline state.

MATERIALS AND METHODS

Preparation of Complexes, Crystallization. Ps. haloplanctis α-amylase, purified as previously described (*4*), and inactive D174N mutant were kindly supplied by Ch. Gerday and G. Feller. Component II and acarbose were provided by Dr. H. Bischoff (Bayer Corp., Wuppertal, Germany).

Native AHA as well as the mutant were crystallized as described previously (*5*) in 60% of 2-methyl-2,4-pentanediol and 0.1 M Tris buffer, using the hanging-drop vapor-diffusion method. Soakings were performed with these crystals in which the enzyme three-dimensional structure showed the presence of a Tris molecule in the active site (*6*) for the wild-type complexes. In the three cases, the soaking time was 30 h at 19 °C, and the final concentrations of component II and acarbose in the droplets was 10 mM.

Collection and Processing of X-ray Diffraction Data. All diffraction data from wild-type AHA crystals soaked with acarbose or component II were collected using synchrotron radiation ($\lambda = 0.9828$ Å) on the D2AM beamline, at the European Synchrotron Radiation Facility (ESRF, Grenoble, France), using a detection system based on a charge-coupled device camera coupled to an image intensifier (*29*). Both data sets were collected at 4 °C using one single crystal in each case. Integration of the data was done with the program XDS (*30*) and further processing with programs from the CCP4 suite (*31*). Data for the inactive mutant complex were collected on a local MARresearch 345 image plate system, using Cu Kα radiation generated from a Nonius FR 591 rotating anode operating at 40 kV and 80 mA with a graphite monochromator. Integration of these data was performed with the program DENZO (*32*) and further processed with programs from the CCP4 package (*31*). Data collection statistics are reported in Table 1.

Table 1: Diffraction Data and Refinement Statistics for the Ternary Complexes of AHA/Tris with Acarbose and Component II, and the Complex of D174N/Acarbose

	acarbose	comp.II	D174N/ acarbose
space group	$C222_1$	$C222_1$	$C222_1$
cell dimensions, Å	$a = 71.01$	$a = 71.33$	$a = 71.1$
	$b = 139.96$	$b = 138.68$	$b = 139.9$
	$c = 115.89$	$c = 114.81$	$c = 115.3$
no. of measurements	110 412	72 535	95 299
no. of unique reflections	45 586	43 621	24 442
resolution, Å	1.74	1.80	2.3
completeness, %	76.6	82.2	95.6
compl. outermost shell[a], %	34.8	54.2	91.1
R_{merge}, %	5.6	6.2	9.2
$I/\sigma(I) > 2$, %	92.8	91.7	100.0
$I/\sigma(I) > 2$ outermost shell[a], %	80.1	89.1	100.0
R_{factor}, %	15.64	16.80	13.8
R_{free}, %	18.73	20.09	18.8
rms deviation from ideal bond length, Å	0.007	0.008	0.008
rms deviation from ideal bond angle, deg	1.66	1.60	1.57
amino acid residues	448	448	448
calcium ions	1	1	1
chloride ions	1	1	1
water molecules	285	274	201

[a] Outermost shells are 1.74−1.83 Å, 1.80−1.90 Å, and 2.30−2.36 Å, respectively. $R_{merge} = \sum_{hkl}\sum_{i=0}^{n}|I_i - \bar{I}_{hkl}|/\sum_{hkl}\sum_{i=0}^{n} I_{ihkl}$. $R_{factor} = \sum_{hkl}|F_o - F_c|/\sum_{hkl}|F_o|$.

Structure Determination and Refinement. To locate the component II and acarbose molecules in the respective complexes, difference electron density maps were generated with phases calculated up to 1.85 Å resolution from the AHA structure in complex with Tris (*6*), (PDB entry code 1AQM), where Tris as well as water molecules in and around the active site had been omitted to prevent any bias. These maps and models were displayed and analyzed using the graphics program TURBO−FRODO (*33*). In all cases, the $2F_o-F_c$ as well as F_o-F_c electron density maps revealed very clearly, and before any refinement, the bound inhibitors. All subsequent refinements were performed using the slowcool procedure, as implemented in X-PLOR version 3843 (*34*), and bulk solvent corrections. A subset of 10% of the data was used to monitor R-free as the procedure progressed. Rounds of refinement were followed by visual inspection of electron density maps coupled with manual model building. Solvent molecules were added to the models if there was unambiguous density in the $2F_o-F_c$ and F_o-F_c maps, appropriate stereochemistry in terms of hydrogen bonding partners, and if refined thermal B-factors were less or equal to 60 Å^2. An analysis of the quality of the refined models is summarized in Table 1.

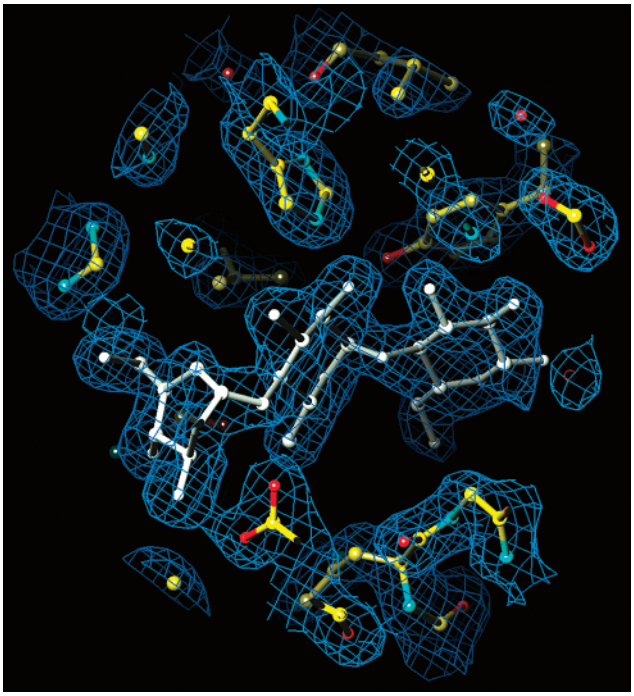

FIGURE 2: $2F_o-F_c$ electron density (contoured at 1σ) map of the AHA/component II complex in the region of the active site. Component II is shown in white.

RESULTS AND DISCUSSION

Structure of the AHA−Component II Complex. The electron density maps calculated on the basis of the 1.8 Å data collected for the AHA/component II complex clearly showed the presence, in the active site and only there, of three rings consistent with the structure of component II (Figure 2). The valienamine part is unambiguously assigned to the sugar-binding subsite −1, whereas the adjacent unit, the 4,6-dideoxyglucose and the glucose rings occupy subsites +1 and +2, respectively (nomenclature according to ref *35*). Binding of component II to AHA does thus not leave any doubt about either the nature or the direction of the sugar rings. It is also very clear that no density is left that could indicate the presence of further sugar rings. In fact, the electron density terminates abruptly at both extremities, indicative of a well-defined trisaccharide species. A large number of interactions (in total 19 hydrogen bonds) occur between the inhibitor and its environment. The average B factors for the three glucosyl moieties (13.8, 15.3, and 22.7 Å^2 for sugars in subsites −1, +1, and +2, respectively) are comparable to those of the surrounding protein residues, suggesting full occupancy of the three sugar binding sites. Their mode of recognition by the enzyme shows general features often observed in protein−carbohydrate interactions (*36*), including hydrogen bonding interactions mediated by water molecules, and will be described and discussed together with the AHA/acarbose complex in the next section.

Structure of the AHA−Acarbose Complex. Contrary to component II, acarbose not only binds to but also reacts with AHA in the crystalline state in a markedly different way. In fact, the corresponding observed electron density map (Figure 3a) clearly suggests the presence of a heptasaccharide compound, the seven sugar rings occupying subsites −4 to +3 and making numerous interactions with the enzyme residues (Figure 3b). The shapes and features of the $2F_o-F_c$ and F_o-F_c electron densities leave no ambiguity on either the direction or the conformation of the reaction product. Subsites −4 to −2 are occupied by sugar moieties constituting a component II molecule, which is further connected to an acarbose moiety, as it corresponds to the best fit possible to the electron density, starting with its nonreducing end at subsite −1 and ending at subsite +3. Subsite +3 corresponds to the reducing end pointing out into the solvent, so it logically appears more mobile than the other sugar rings in accordance with the observed values of their refined average thermal B-factors: from subsites −4 to +3 these values (corresponding values for component II are given within parentheses) are 42.2; 17.6; 11.3; 9.9 (13.8); 10.7 (15.3); 18.5 (22.7); 38.5 Å^2. When comparing the active sites of the two AHA complexes, the three rings of component II superimpose almost perfectly onto the corresponding units of acarbose in the complex with AHA.

In other acarbose-based complexes with PPA isozyme I (*20*), with α-amylase from *Aspergillus oryzae* (*23*), the maltogenic α-amylase from *Bacillus stearothermophilus* (*25*), and human pancreas α-amylase (*26*), no binding at subsite −4 was observed, whereas the complexes between acarbose and PPA (isozyme II) as well as the complex with a chimeric bacterial α-amylase, BA2, (*27*) showed the presence of a valienamine ring at subsite −4 (*21*), as found in the present study. In contrast, the structure of barley α-amylase (isozyme II) interacting with acarbose reveals well defined and continuous electron density consistent with the presence of only three sugar rings, suggesting that the glucose unit at the reducing end of the tetrasaccharide was cleaved off through hydrolysis in the crystal, leading to a bound component II molecule (*24*).

The Active Site Region Binds Two Competitive Inhibitors. It is known that Tris competitively inhibits several glycosidases (*37*−*40*) including α-amylases (*6*, *27*). The first three-dimensional structure of wild-type AHA was shown to incorporate in the active site a Tris molecule that interacts via very strong hydrogen-bonding interactions with all of the three essential catalytic residues, Asp 174, Glu 200, and Asp 264 (*6*), suggesting again that Tris is an ideal molecule tailored for binding to an α-amylase active site.

The electron density maps of the two native complexes are consistent with the fact that, although the Tris molecule is driven out of the active site by the incoming oligosaccharide inhibitor, it stays in the immediate environment, and in hydrogen bonding contact with component II or acarbose (Figure 3b). The new Tris binding sites are therefore completely different from the original position seen in the Tris inhibited AHA structure: in the AHA/component II complex, Tris is displaced by 7 Å and binds via its nitrogen atom to the nonreducing end (subsite −1) of the inhibitor, whereas in the AHA/acarbose complex, it shifts by 9 Å to interact via one of its hydroxyl groups with an inhibitor glucose hydroxyl in subsite +2 and via another of its hydroxyl groups to an inhibitor glucose hydroxyl in subsite −2 (Figure 3b). In the latter complex, no interactions are performed with the Tris nitrogen atom.

Although oligosaccharide inhibitor binding to AHA induces large displacements of the Tris molecule, remarkably, in each case Tris remains bound to the incoming inhibitor, although via different interaction schemes. Despite its very strong electrostatic interactions with the highly negatively

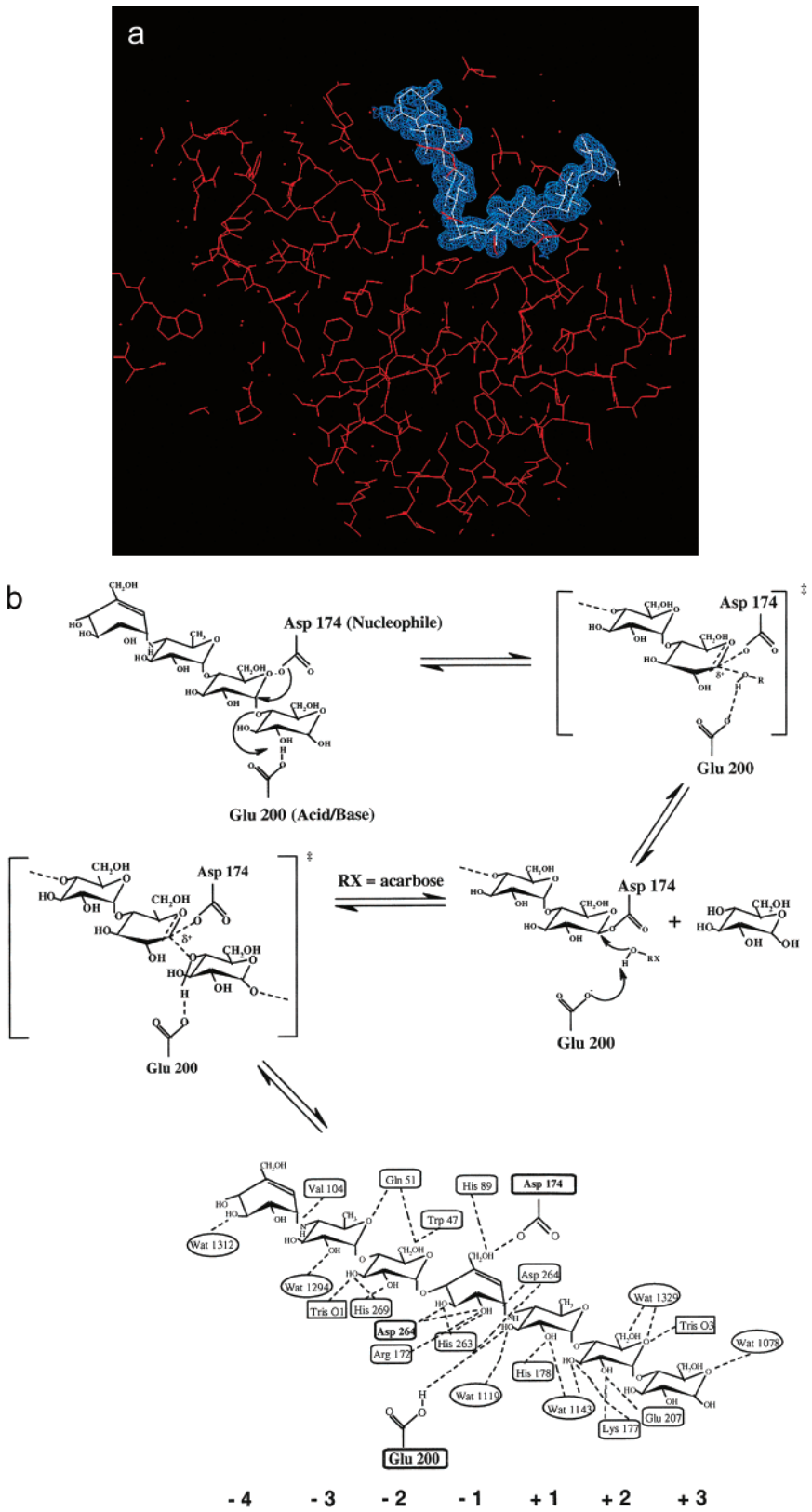

FIGURE 3: (a) $2F_o-F_c$ electron density map (contoured at 1σ), showing the heptasaccharide in white, bound in the active site of AHA represented in red. (b) Transglycosylation reaction for AHA leading to the heptasaccharide, and a schematic drawing of the hydrogen bonding interactions between this acarbose-derivative and AHA, Tris, and water molecules. The subsites positions of the respective sugar rings are indicated at the bottom, according to the nomenclature (*35*).

charged AHA active site, Tris is pushed out by the new incoming substrate analogue. This can now be easily understood when comparing the number and nature of interactions performed by each ligand and can be correlated to its specific affinity with AHA, including bonds with water molecules, Tris makes a total of 7 hydrogen bonds with its environment (in the AHA/Tris complex), compared to 19 for component II and 31 for the heptasaccharide (Figure 3b).

To our knowledge, these are the first observations of competition, in the crystalline state, between two inhibitors present in the active site region of an enzyme.

Besides the considerable Tris movements, comparison of the structures of native AHA, of AHA in complex with Tris or with acarbose-like molecules reveals not only the structural features that contribute to the binding of the oligosaccharide inhibitor substrate analogues but also the conformational changes induced by their interactions with the enzyme.

Overall, there are no major differences between the various AHA three-dimensional structures. However, significant shifts that accompany binding of acarbose concern the glycine-rich loop with residues 268−273, in the immediate vicinity of the active site. This loop movement, which is not observed in the AHA/Tris nor in the AHA/component II complexes, involves a shift of about 2.6 Å for His 269 (distance between the ND1's) to form hydrogen bonding interactions with both the Tris and oligosaccharide moieties, whereas Gly 270 moves by 2.4 Å.

A similar and even more flexible glycine-rich loop (304−309 in PPA) was observed upon acarbose (or acarbose-like compound) binding in the three-dimensional structures of the complexes with porcine pancreas (*20*−*22*) and human pancreas α-amylase (*26*). It already has been suggested (*20*) that movement of this loop may have a functional significance, as it restricts access to the active site and may partially protect the bound reaction products from the solvent. Furthermore, when this loop returns to its original position, it may favor the release of products by disruption of their interactions with the enzyme. These views are reinforced with the present observations. Finally, we here demonstrate that this loop movement is not observed and in fact is not required in AHA when it just binds, without consecutive processing, shorter substrate analogues such as component II, or small inhibitors such as the Tris molecule.

AHA Catalytic Mechanism. α-Amylases, like all the retaining glycosidic hydrolases from family 13, perform general acid−base type of catalysis with a net retention of anomeric configuration (*41*) via a double displacement mechanism as originally proposed (*42*), involving two carboxylic acid residues of which one serves as the acid−base catalyst and the other as the nucleophile that stabilizes the glycosyl−enzyme reaction covalent intermediate. In AHA, the proton donor and catalytic nucleophile have been proposed as being Glu 200 and Asp 174, respectively, based on sequence similarity with other α-amylases, on unambiguous detection of covalent glycosyl intermediates in other glycosyl hydrolases of family 13 (*43*−*46*), and on the 3D structure of Tris-complexed AHA (*6*).

The interaction pattern involving the heptasaccharide reaction product bound to AHA (Figure 3b) confirms the functions of the various amino acids important for recognition and/or hydrolysis of a substrate. In the first step of the hydrolytic reaction, Glu 200 makes a hydrogen bond to the interglycosidic oxygen atom between the two glucose moieties in the acarbose, an atom that would correspond to the position of the interglycosidic oxygen of a true substrate, between subsites −1 and +1. This will result in a transition state having substantial oxocarbenium character and allowing the departure of the leaving reducing end group, followed by a nucleophilic attack by Asp 174 on the anomeric C1 atom, a reaction leading to a covalent glycosyl-intermediate

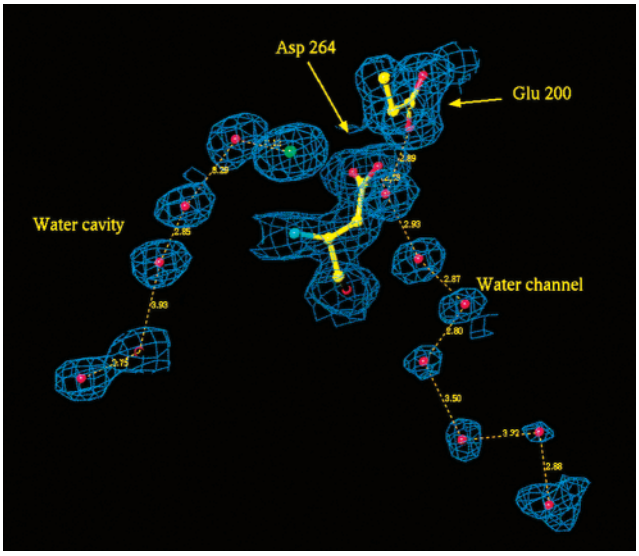

FIGURE 4: The water cavity and the substrate-induced water channel with the "hydrolytic" water (Wat 1004) bridging Glu 200 and Asp 264, as seen in the AHA/acarbose complex. The chloride effector ion (green dot) is bound to the water cavity and the water channel runs from the active site through the enzyme to the surface (see also Figure 5).

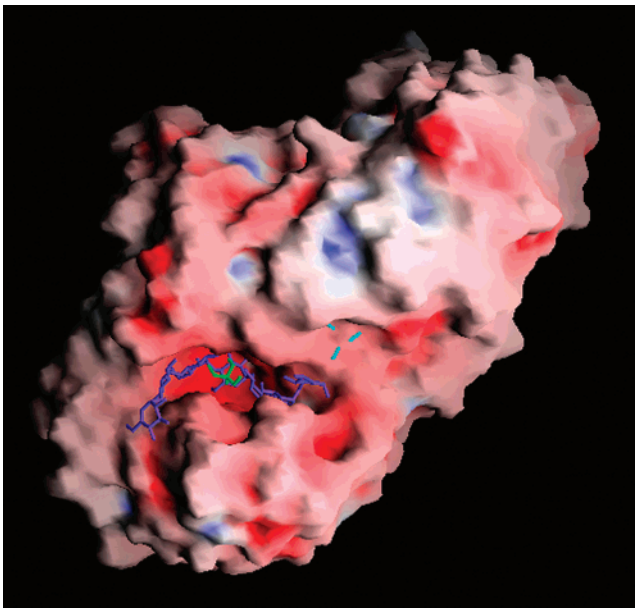

FIGURE 5: The electrostatic surface potential of the AHA complex visualized using Grasp (*11*). Regions of positive potential are shown in blue, and negative potential is in red. The active site region accommodates two inhibitors, the heptasaccharide (in purple) resulting from the transglycosylation of acarbose and the Tris molecule (in green). The channel (seen in Figure 4) starts at the surface with three well ordered water molecules (in blue sticks).

with inverted configuration of the anomeric carbon. After cleavage of the scissile bond, an acceptor comes in, which in case of hydrolysis would be a water molecule, or as here a carbohydrate C4-hydroxyl group if transglycosylation is taking place. Glu 200 then acts as a general base, activating the acceptor group through deprotonation: in the case of hydrolysis, this group could be the so-called "hydrolytic" water (Wat 1004), which is of special interest as it bridges Asp 264 and Glu 200 (Figure 5) (*6*), as suggested also previously for barley α-amylase (*24*). The resulting hydroxide ion performs nucleophilic attack at C1 with formation

of a reaction product of overall retained configuration. Movement of this hydroxide ion is most probably promoted by the electrostatic repulsive field created by the nearby chloride ion, and by the negatively charged surrounding side chains.

A Transglycosylation Reaction Occurs in the Crystal. It is known that glycosidases, and among them α-amylases, can display transglycosylation activity (*47*−*49*). This means that these enzymes are able to rearrange the cleavage products, resulting in the formation of extended oligosaccharide species that can undergo further processing. In the case of α-amylases, the glycosyl covalent reaction intermediate that is formed is deglycosylated by an incoming water molecule acting as a nucleophile, but an alternate scheme (transglycosylation) that involves an oligosaccharide moiety instead of water to attack the sugar substrate will lead to a longer sugar chain. For example, PPA can realize successive events, like hydrolysis, transglycosylation, and condensation, depending on the nature of the substrate and its concentration (*47*). Indeed, a number of glycosidases are used in synthetic chemistry for producing oligosaccharides by transglycosylation (*48*, *50*).

That various α-amylases (or related amylolytic enzymes) are able to process the initially added acarbose to larger products, considered as more potent inhibitors, has been suggested by several recent crystallographic studies and strongly supports the transglycosylation activity taking place in the crystals of these enzymes (*20*, *21*, *23*, *25*−*27*, *51*). The AHA/acarbose complex reveals an extended binding site much longer than expected for a single acarbose molecule. We have shown that careful interpretation of the corresponding unbiased electron density maps, followed by subsequent simulated annealing refinement cycles, allowed unambiguous identification of the species bound in the active site of AHA. Furthermore, detailed comparisons with the structure of the AHA/component II complex and with previous structural findings on other α-amylase/acarbose systems (*20*, *21*, *23*−*28*) helped us to conclude that the bound sugar chain does not correspond to an overlapping network of tetrasaccharides, but is a well-defined heptasaccharide due to an enzymatic transglycosylation event. This reaction can be explained straightforward: first, a molecule of acarbose binding in subsites −3, −2, −1, and +1 is cleaved with liberation of glucose and formation of a trisaccharide glycosyl−enzyme intermediate, which further is deglycosylated by a second acarbose molecule playing the role of acceptor; with the nucleophilic attack by this acarbose moiety the component II unity, already present in the active site of AHA, is pushed toward the nonreducing end, and the acarviosine unit of the newly incoming acarbose is now present in subsites −1 and +1. Then, because the interglycosidic nitrogen atom is situated at the cleavage point, no further hydrolysis and/or transglycosylation is possible. This process therefore generates a heptasaccharide species formed by a component II unit covalently linked to an acarbose molecule (Figure 3b).

To definitely support that transglycosylation can occur in the AHA crystals, site-directed mutagenesis was also used to change one of the catalytic important residues. Among the latter, Asp 174 (the nucleophile) was mutated into Asn, and this mutant could be crystallized. Its 3D structure was determined at 2.3 Å resolution, as well as that of its complex with acarbose, prepared under the same conditions as those

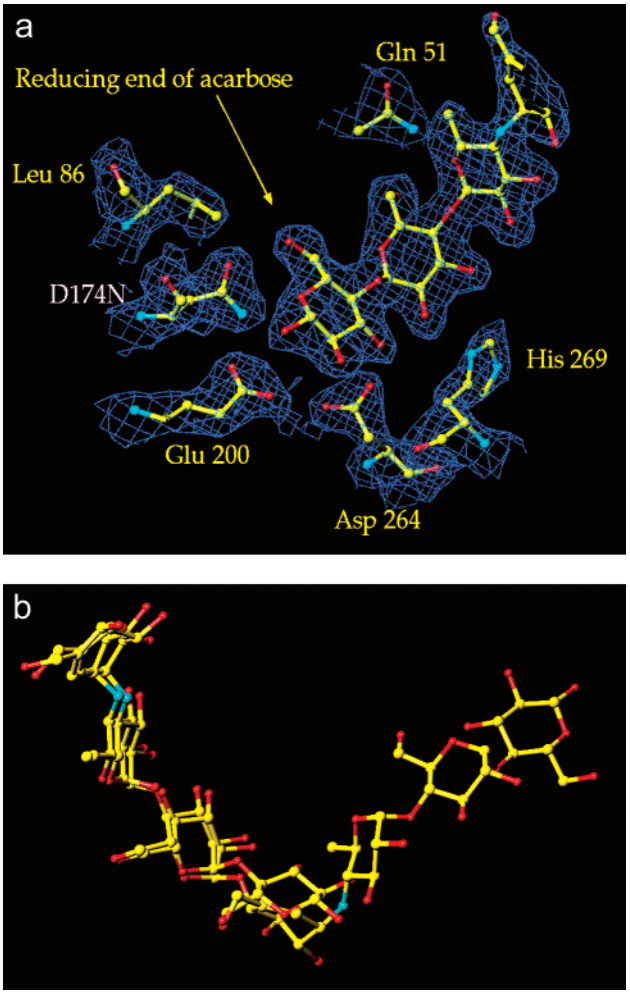

FIGURE 6: (a) $2F_o-F_c$ electron density map (contoured at 1σ), showing the acarbose molecule bound in the active site of D174N (b) Superimposition of the active site region of the active enzyme with the bound heptasaccharide and the inactive enzyme with acarbose bound. Acarbose is occupying subsites −4 to −1.

leading to the above-described wild-type AHA/acarbose complex (see Materials and Methods). This mutation abolishes enzyme activity, as expected, and does not induce any significant conformational change as established by the X-ray crystal structure of the mutant. Moreover, the electron density map of the mutant complex is fully consistent with a very well-defined single acarbose molecule binding in a nonproductive way to the active site region in subsites −4 to −1, and only there (Figure 6), confirming that no transglycosylation has taken place. Therefore, the hypothesis of two acarbose overlapping binding sites that was put forward to explain the extended electron density observed in the AHA and other α-amylases in complex with acarbose is clearly no longer valid.

Finally, in view of the above results, it is tempting to suggest that in all α-amylases mutation of the residue functioning as the nucleophile in the catalytic mechanism will not prevent binding of substrate-analogues such as acarbose-like molecules, but will abolish not only the hydrolysis but also the transglycosylation events.

A Channel with Substrate-Induced Ordering of Water Molecules. Upon acarbose binding to AHA, a chain of seven very well defined ordered water molecules appears in the active site (Figure 4). More precisely, these water molecules

mark a channel leading from Wat 1004 in the active site (just behind the interglycosidic bond to be cleaved) to Wat 1370 situated at the surface of the enzyme (Figure 4, Figure 5). Interestingly, Wat 1004 (strictly conserved in all known α-amylase 3D structures) at the starting point of this water channel corresponds to the so-called "hydrolytic" water molecule, as it is suggested to be implicated in the hydrolysis performed by at least AHA and barley α-amylases, as discussed previously (*6*, *24*). Remarkably, none of these water sites (except Wat 1004) were observed in the native wild-type, nor in the native recombinant and in the Tris-bound AHA structures. Taking into account that hydrolysis of acarbose by α-amylase leads to cleavage of the glucose unit from the reducing end (*24*, *52*), it is tempting to propose that the channel possibly might serve as a water supply for ensuring substrate hydrolysis. This point is even reinforced by the fact that this channel ends at the surface of the enzyme, and thus has direct access to the bulk solvent (Figure 5).

In the complex between barley α-amylase isozyme 2 and acarbose (as well as in the native enzyme structure) a buried cavity containing a chain of six ordered water molecules was observed and proposed to function as a reservoir implicated in the hydrolytic reaction of the substrate (*24*, *53*). However, and interestingly, this water chain, in terms of its spatial location, does not correspond to the above channel found in the ternary complexes of AHA, and moreover, it has no access to the bulk solvent. In fact, such a water chain is also observed in the AHA (*6*) and the known mammalian α-amylase structures (native and complexes) where it is situated behind and linked to the activator chloride ion (Figure 4). It is striking that the two water molecule networks that form the buried water pocket and the open water channel converge near the site of the "hydrolytic" water molecule, Wat 1004 bridging Glu 200 and Asp 264 (Figure 4), whereas the extremities of the two networks are 19 Å from one another. In structural investigations of the complex between PPA (also a chloride activated α-amylase) and a thio-oligosaccharide inhibitor, a similar water structure was observed, but no role was assigned to it (*54*). We suggest that such an ordering of water molecules in a channel is a feature characteristic of the α-amylase/substrate 3D structures and is used in the catalytic process**.** This conclusion is reinforced by the absence of "like" ordered water molecules in the complex between the inactive mutant and acarbose, suggesting that if binding occurs without subsequent reaction, these "channel water molecules" are not needed and highly disordered. Of course, care should be taken when making conclusions about water molecules at 2.3 Å resolution, but the electron density maps, $2F_o-F_c$ as well as F_o-F_c are indeed very clear.

In conclusion, the crystal structures of the AHA/oligosaccharide complexes reveal both conserved and unique features in comparison with other α-amylase systems. Common to the other α-amylases, AHA displays an active site capable of binding a polysaccharide via an intricate pattern of interactions that appears highly similar to that seen in all known amylolytic enzymes, even concerning a number of water molecules mediating the inhibitor/enzyme association. Surprisingly, in many aspects the resemblance of this bacterial psychrophilic α-amylase is greatest with its mesophilic mammalian α-amylase counterparts, and the present AHA structures confirm the crucial role of some amino acids for recognition and substrate processing. However, there are remarkable differences in the way in which AHA recognizes and transforms the well-known glycosidase tetrasaccharide inhibitor, acarbose. First, acarbose expels the prebound inhibitor Tris from the active site, but keeps it bound in forming a well-defined ternary complex. Second, the reaction product, which is a heptasaccharide species, can be considered as a better inhibitor of AHA, resulting from a transglycosylation event in the crystal. This is the first observation of such an extended oligosaccharide produced by an α-amylase, a compound that appears to be the logical consequence of the enzyme transglycosylation ability, as suggested and predicted (but not observed before) for the reaction between the fungal TAKA-amylase and acarbose (*23*).

Third, the complex between the inactive mutant, D174N, and acarbose in which the substrate analogue is recognized but not transformed, clearly proves that not only is the native cold adapted α-amylase active in the crystalline state, but it also performs a transglycosylation reaction that is abolished, as expected, in the crystals of the inactive mutant. The question that remains to be answered is why binding only occurs in subsites −4 to −1. Fourth, the acarbose substrate analogue binding to AHA reveals a channel filled with ordered water molecules, which were not observed in the native nor in the Tris inhibited structures of AHA. This channel may well have at least a dual role: besides its primary function of providing water for the hydrolytic reaction and regulating water movement through the active site, it may also provide an exit mechanism for water molecules that are displaced upon binding of the substrate, as suggested also in other systems (*55*). It provides the "hydrolytic" water molecule binding to the essential glutamic side chain which is proposed to have several important functions: proton donation to the interglycosidic oxygen of the substrate, activation (together with the chloride effector ion) of the "hydrolytic" water, and stabilization of the sugar ring adjacent to the cleavage site. Appropriate mutants, designed to modify the channel structure in view of preventing water movements and of causing an eventual reduction of the enzyme activity, may help to elucidate the function of this channel.

Furthermore, the present AHA structures can also contribute to provide a basis for structure-based drug design in the field of glycosidase inhibitors. The heptasaccharide described in this paper enlarges the list of glycosidase inhibitors, some of which have already moved out of the laboratory and into the clinic as potential agents for the treatment of diseases including diabetes and hyperlipaemia (*56*). Therefore, besides acarbose, which is already marketed as (Glucor), there is a rationale for exploring a role for more α-glucosidase inhibitors, for finding additional pharmacophores that will increase the chance of identifying even better antidiabetic drugs in terms of both efficiency and/or lack of adverse side effects.

Finally, it is worth recalling that AHA, like all enzymes from organisms adapted to cold environments, functions optimally at low temperature and has therefore significant potential in biotechnological applications (*57*, *58*). Therefore, the present AHA models appear very useful in engineering other active-site mutants, as well as mutants with various transglycosylation possibilities and/or with enhanced stability without loss of catalytic efficiency in cold environments.

ACKNOWLEDGMENT

We thank H. Bischoff (Bayer AG) for supplying acarbose and component II, G. Feller for preparing and providing wild-type and mutant enzyme for the crystallographic studies, and P. Legrand for assistance with data collection at ESRF.

REFERENCES

1. Vihinen, M., and Mäntsälä, P. (1989) *Crit. Rev. Biochem. Mol. Biol. 24*, 329−418.
2. Dong, G., Vieille, C., Savchenko, A., and Zeikus, J. G. (1997) *Appl. Environ. Microbiol. 63*, 3569−76.
3. Bauer, M. W., Driskill, L. E., and Kelly, R. M. (1998) *Curr. Opin. Biotech. 9*, 141−145.
4. Feller, G., Lonhienne, T., Deroanne, C., Libioulle, C., Van Beeumen, J., and Gerday, C. (1992) *J. Biol. Chem. 267*, 5217−21.
5. Aghajari, N., Feller, G., Gerday, C., and Haser, R. (1996) *Protein Sci. 5*, 2128−9.
6. Aghajari, N., Feller, G., Gerday, C., and Haser, R. (1998) *Protein Sci. 7*, 564−72.
7. Aghajari, N., Feller, G., Gerday, C., and Haser, R. (1998) *Structure 6*, 1503−16.
8. Strobl, S., Maskos, K., Wiegand, G., Huber, R., Gomis-Ruth, F. X., and Glockshuber, R. (1998) *Structure 6*, 911−21.
9. Feller, G., Bussy, O., Houssier, C., and Gerday, C. (1996) *J. Biol. Chem. 271*, 23836−41.
10. D'Amico, S., Gerday, C., and Feller, G. (2000) *Gene 253*, 95−105.
11. Nicholls, A. (1993) *Biophys. J. 64*, A116.
12. Aghajari, N. (1998) pp 1−232, Ph.D. Thesis, Université d'Aix Marseille II & Université de Liège.
13. Feller, G., Bussy, O., Houssier, C., and Gerday, C. (1996) *J. Biol. Chem. 271*, 23836−41.
14. Schmidt, D. D., Frommer, W., Junge, B., Muller, L., Wingender, W., Truscheit, E., and Schafer, D. (1977) *Naturwissenschaften 64*, 535−6.
15. Schmidt, D. D., Frommer, W., Junge, B., Müller, L., Wingender, W., and Truscheit, E. (1981) in *First International Symposium on Acarbose* (Creutzfeldt, W., Ed.) pp 5−15, Excerpta Medica, Amsterdam.
16. Schmitt, E. W. (1987) In *A New Principle in the Treatment of Diabetes Mellitus: Alpha-Glucosidase Inhibition of Acarbose* (Bayer AG, Ed.), Leverkussen, Germany.
17. Clissold, S. P., and Edwards, C. (1988) *Drugs 35*, 214−43.
18. Brogard, J. M., Willemin, B., Blicklé, J. F., Lamalle, A. M., and Stahl, A. (1989) *Rev. Med. Interne 10*, 365−374.
19. Bischoff, H., Ahr, H. J., Schmidt, D., and Stoltefuss, J. (1994) *Nachr. Chem. Tech. Lab. 42*, 1119−1128.
20. Qian, M., Haser, R., Buisson, G., Duee, E., and Payan, F. (1994) *Biochemistry 33*, 6284−94.
21. Gilles, C., Astier, J. P., Marchis-Mouren, G., Cambillau, C., and Payan, F. (1996) *Eur. J. Biochem. 238*, 561−9.
22. Machius, M., Vertesy, L., Huber, R., and Wiegand, G. (1996) *J. Mol. Biol. 260*, 409−21.
23. Brzozowski, A. M., and Davies, G. J. (1997) *Biochemistry 36*, 10837−45.
24. Kadziola, A., Sogaard, M., Svensson, B., and Haser, R. (1998) *J. Mol. Biol. 278*, 205−17.
25. Dauter, Z., Dauter, M., Brzozowski, A. M., Christensen, S., Borchert, T. V., Beier, L., Wilson, K. S., and Davies, G. J. (1999) *Biochemistry 38*, 8385−92.
26. Brayer, G. D., Sidhu, G., Maurus, R., Rydberg, E. H., Braun, C., Wang, Y., Nguyen, N. T., Overall, C. M., and Withers, S. G. (2000) *Biochemistry 39*, 4778−91.
27. Brzozowski, A. M., Lawson, D. M., Turkenburg, J. P., Bisgaard-Frantzen, H., Svendsen, A., Borchert, T. V., Dauter, Z., Wilson, K. S., and Davies, G. J. (2000) *Biochemistry 39*, 9099−107.
28. Qian, M., Nahoum, V., Bonicel, J., Bischoff, H., Henrissat, B., and Payan, F. (2001) *Biochemistry 40*, 7700−9.
29. Moy, J.-P. (1994) *Nucl. Instrum. Methods Phys. Res. A348*, 641−644.
30. Kabsch, W. (1993) *J. Appl. Crystallogr. 26*, 795−800.
31. CCP4 (1994) *Acta Crystallogr. D Biol. Crystallogr. 50*, 760−763.
32. Otwinowski, Z., and Minor, W. (1997) in *Methods in Enzymology, Macromolecular Crystallography, Part A* (Carter, C. W., and Sweet, R. M., Eds.) pp 307−326, Academic Press, London and New York.
33. Roussel, A., and Cambillau, C. (1989) in *Silicon Graphics Geometry Partners Directory* (Graphics, S., Ed.) pp 77−78, Silicon Graphics, Mountain View, California.
34. Brünger, A. T. (1997) pp 366−396.
35. Davies, G. J., Wilson, K. S., and Henrissat, B. (1997) *Biochem. J. 321*, 557−9.
36. Vyas, N. K. (1991) *Curr. Opin. Struct. Biol. 1*, 723−740.
37. Myrbäck, K. (1965) *Arkiv Kemi 30*, 315−320.
38. Jorgensen, B. B., and Jorgensen, O. B. (1967) *Biochim. Biophys. Acta 146*, 167−72.
39. Kersters-Hilderson, H., Loontiens, F. G., Claeyssens, M., and De Bruyne, C. K. (1969) *Eur. J. Biochem. 7*, 434−41.
40. Chen, C. C., Guo, W. J., and Isselbacher, K. J. (1987) *Biochem. J. 247*, 715−24.
41. McCarter, J. D., and Withers, S. G. (1994) *Curr. Opin. Struct. Biol. 4*, 885−92.
42. Koshland, D. E. (1953) *Biol. Rev. 28*, 416−436.
43. Braun, C., Brayer, G. D., and Withers, S. G. (1995) *J. Biol. Chem. 270*, 26778−81.
44. McCarter, J. D., and Withers, S. G. (1996) *J. Biol. Chem. 271*, 6889−94.
45. Uitdehaag, J. C., Mosi, R., Kalk, K. H., van der Veen, B. A., Dijkhuizen, L., Withers, S. G., and Dijkstra, B. W. (1999) *Nat. Struct. Biol. 6*, 432−6.
46. Uitdehaag, J. C., van Alebeek, G. J., van Der Veen, B. A., Dijkhuizen, L., and Dijkstra, B. W. (2000) *Biochemistry 39*, 7772−80.
47. Robyt, J. F., and French, D. (1970) *J. Biol. Chem. 245*, 3917−27.
48. Nilsson, G. I. (1988) *Trends Biotechnol. 6*, 256−264.
49. Matsui, I., Yoneda, S., Ishikawa, K., Miyairi, S., Fukui, S., Umeyama, H., and Honda, K. (1994) *Biochemistry 33*, 451−8.
50. Terashima, M., and Katoh, S. (1996) *Ann N.Y. Acad. Sci. 799*, 65−9.
51. Strokopytov, B., Penninga, D., Rozeboom, H. J., Kalk, K. H., Dijkhuizen, L., and Dijkstra, B. W. (1995) *Biochemistry 34*, 2234−40.
52. Müller, L., Junge, B., and Frommer, W. (1980) in *Enzyme inhibitors* (Brodbeck, U., Ed.) pp 109−122, Verlag Chemie, Weinheim.
53. Kadziola, A., Abe, J., Svensson, B., and Haser, R. (1994) *J. Mol. Biol. 239*, 104−21.
54. Qian, M., Spinelli, S., Driguez, H., and Payan, F. (1997) *Protein Sci. 6*, 2285−96.
55. Humm, A., Fritsche, E., Steinbacher, S., and Huber, R. (1997) *EMBO J. 16*, 3373−85.
56. Jacob, G. S. (1995) *Curr. Opin. Struct. Biol. 5*, 605−11.
57. Feller, G., and Gerday, C. (1997) *Cell Mol. Life Sci. 53*, 830−841.
58. Russell, N. J. (1998) *Adv. Biochem. Eng. Biotechnol. 61*, 1−21.

BI0160516